Electronic Supplementary Material (ESI) for Dalton Transactions.

Electronic Supplementary Information (ESI)

Rationally designed curcumin based ruthenium(II) antimicrobials effective against drug-resistant *Staphylococcus aureus*

Payal Srivastava,[a] Manjulika Shukla,[§b] Grace Kaul,[§b] Sidharth Chopra*[b] and Ashis K. Patra*[a]

[a] Department of Chemistry, Indian Institute of Technology Kanpur, Kanpur 208016, Uttar Pradesh, India

[b] Division of Microbiology, CSIR-Central Drug Research Institute, Lucknow 226031, Uttar Pradesh, India

Experimental

Synthesis

The synthesis and characterization of complexes $[Ru(NN)_2(cur)](PF_6)$ [NN= bpy (**1**), phen (**2**)] were given in the main paper.

Synthesis of $[Ru(bpy)_2(acac)](PF_6)$ (3)

A modified procedure is used for the synthesis of Complex **3** used as control compound.[S1] $[Ru(bpy)_2Cl_2]$ (0.124 g, 0.25 mmol) was dissolved in ethanol (7 mL), acetylacetone (0.025 g, 0.25mmol) was added, followed by triethylamine (0.026 g, 0.25mmol) and the mixture was refluxed for 12 h. The reaction mixture was filtered, concentrated to half of its volume and ammonium hexafluorophosphate (NH_4PF_6) (0.167 g, 1mmol) was added to give a black purple coloured powder. The product was filtered and washed with Et_2O (2 x 3 mL) and dried under vaccum. Yield: 0.142 g (81%). Anal. Calcd for $C_{25}H_{23}F_6N_4O_2P_1Ru_1$: C, 45.67; H, 3.53; N, 8.52; Found: C, 44.41; H, 3.46; N, 9.28. FT-IR (KBr, ν_{max}, cm^{-1}): 3438 (m, br), 3077 (w), 2923 (w), 1630 (w), 1603 (w), 1566 (s) (C=O stretching), 1519 (s), 1463 (m), 1445 (s) (C=C stretching), 1423 (m), 1309 (w), 1265 (w), 1241 (w), 1213 (w), 1023 (m), 933 (w), 878 (w), 837 (vs)(P-F stretching, PF_6), 762 (s), 730(m), 659 (w), 615 (w), 557 (m), 424 (w) (vs, very strong; s, strong; m, medium; w, weak; br, broad). ESI-MS (*m/z*) in EtOH: $[M\text{-}PF_6]^+$ calcd: 513.09 (100.0%), 512.09 (53.8%), 515.09 (59.2%), 511.09 (39.9%), 510.09 (40.2%), 514.09 (27.0%). Found: 513.09 (100.0%), 512.09 (51.0%), 515.09 (47.2%), 511.09 (36.9%), 510.09 (30.8%), 514.09 (21.4%).

Synthesis of $[Ru(phen)_2(acac)](PF_6)$ (4)

Complex **4** was prepared using similar method to complex **3** except reacting with $[Ru(phen)_2Cl_2]$ (0.133 g, 0.25 mmol). Yield: 0.144g (78 %) Anal. Calcd for $C_{29}H_{23}F_6N_4O_2P_1Ru_1$: C, 49.37; H, 3.29; N, 7.94; Found: C, 52.62; H, 3.07; N, 10.09. FT-IR (KBr, ν_{max}, cm^{-1}): 3431 (m, br), 3066

(w), 1974 (w), 1698 (w), 1629 (w), 1556 (m) (C=O stretching), 1516 (m), 1446 (w), 1428 (s) (C=C stretching), 1397 (m), 1340 (w), 1290 (w), 1266 (w), 1248 (w), 1223 (w), 1202 (w), 1148 (w), 1097 (w), 1052 (w), 1025 (w), 915 (w), 877 (w), 841 (vs) (P-F stretching, PF_6), 795 (w), 772 (w), 734 (w), 719 (m), 622 (w), 611 (w), 558 (m), 537 (w), 525 (w), 495 (w), 448 (w) (vs, very strong; s, strong; m, medium; w, weak; br, broad). ESI-MS (*m/z*) in EtOH: $[M\text{-}PF_6]^+$ calcd: 561.09 (100.0%), 560.09 (53.8%), 563.09 (59.2%), 559.09 (39.9%), 558.09 (40.2%), 562.09 (31.4%). Found: 561.09 (100.0%), 560.09 (51.0%), 563.09 (45.4%), 559.09 (37.6%), 558.09 (28.5%), 562.09 (22.9%).

Solubility. The complexes (**1**-**4**) were soluble in acetone, alcohol, acetonitrile, chloroform, dichloromethane, dimethylformamide and dimethyl sulfoxide.

X-ray Crystallographic Procedure

X-ray single crystals were obtained by vapour diffusion of diethylether on to the DCM solution of the complexes **1** and **2**. Single crystal of suitable dimension was mounted on a glass fiber and used for data collection. All geometric and intensity data were collected on a Bruker D8 Quest Microfocus X-ray CCD diffractometer equipped with an Oxford Instruments low-temperature attachment, with graphite-monochromated Mo Kα radiation (λ =0.71073 Å) at 100(2) K using the ω-scan technique (width of 0.5° per frame) at a scan speed of 10 s per frame controlled by manufacturer's APEX2 v2012.4-3 software package.[S2] The structures were solved by using direct methods in SHELXS-97 and was refined on F^2 by using a full-matrix least-squares technique in SHELXL-97.[S3,S4] Selected crystallographic data and refinement parameters for the complex are summarized in Table S1. Selected bond distances and angles for all the complexes are given in Table S2.

DNA Binding experiments

The DNA binding experiments of the ruthenium(II) complexes (**1** and **2**) were studied by UV-vis absorption titration and ethidium bromide (EB) displacement assay.

Absorption spectral studies

The interaction of the ruthenium complexes with CT-DNA were studied using UV-vis absorption titration in 5 mM Tris-HCl/NaCl buffer (pH 7.2) using complexes **1** and **2**. The DNA concentrations were determined from the absorption intensity at 260 nm with $\varepsilon = 6600\ M^{-1}\ cm^{-1}$. The absorption titration experiments were performed using a varying concentration of CT DNA while keeping the concentration of metal complex (27 μM) as constant. During each measurement, an equilibration of 3 min was given and absorbance change was recorded. The intrinsic equilibrium binding complex (K_b) of the ruthenium complexes to CT DNA was determined by the following equation:[S5]

$$[DNA]/(\varepsilon_a - \varepsilon_f) = [DNA]/(\varepsilon_b - \varepsilon_f) + 1/K_b(\varepsilon_b - \varepsilon_f)$$

where [DNA] is the concentration of CT DNA in the base pairs, ε_a is the apparent extinction coefficient, ε_f and ε_b refers to the extinction coefficients of the complex in its free and fully bound form. The K_b values were obtained from the linear plot of $[DNA]/(\varepsilon_a - \varepsilon_f)$ vs.[DNA].

Ethidium bromide (EB) displacement assay

The competitive binding ability of the complexes **1** and **2** was measured through ethidium bromide displacement assay in 5 mM Tris-HCl/NaCl buffer (pH, 7.2). The quenched emission spectra of free EB shows enhanced emission peak on intercalating with CT DNA at 605 nm (λ_{ex}= 546 nm). The complexes were titrated into the DNA bound EB mixture and significant changes in the emission intensity were noted. The apparent binding constant (K_{app}) was determined by the following equation:[S6]

$$K_{app} \times C_{50} = K_{EB} \times [EB]$$

where K_{app} is the apparent binding constant of the complexes, C_{50} is the concentration of the complex at 50% reduction of fluorescence intensity of EB. K_{EB} is the binding constant of the EB ($K_{EB} = 1.0 \times 10^7\ M^{-1}$), and [EB] is the concentration of ethidium bromide.

Protein binding studies

The protein binding study of the complexes were studied using tryptophan emission quenching experiments in 5 mM Tris–HCl/NaCl buffer (pH 7.2) keeping the concentration of HSA (2 μM)

constant and gradually increasing the complex concentration (1-19 μM) at λ_{ex} = 295 nm. The quenching constant (K_{HSA}) was determined quantitatively using Stern-Volmer equation,[S7]

$I_0 / I = 1 + k_q\tau_0[Q] = 1 + K[Q]$

where I_0 and I are the steady-state emission intensities of HSA in the absence and presence of quencher of concentration [Q] and K is the Stern-Volmer quenching constant for HSA, k_q is the quenching rate constant, τ_0 the average lifetime of the biomolecule without quencher (~10^{-8} s). Hence, K was obtained from slope of the linear regression of a plot of I_0/I against [Q]. The type of quenching involved between protein and complexes is represented by the Scatchard equation,[S8]

$\log(I_0 - I) / I = \log K + n\log[Q]$, where K is the binding constant of the complex with protein and n is the number of binding sites. The plot of log $(I_0 - I)/I$ versus log[Q] yields a straight line of slope (n) and negative intercept (K) on X-axis.

Antibiotic susceptibility testing

Antibiotic susceptibility testing was carried out according to the CLSI guidelines for broth microdilution assay.[S9] 10 mg/mL stock solutions of test compounds were prepared in DMSO. Bacterial cultures were inoculated in MHB and optical density (OD) of the cultures was measured at the 600 nm wavelength, followed by dilution to achieve ~10^5 CFU/mL. The compounds were tested ranging from 64-0.5 mg/L in two-fold serial diluted fashion with 2.5 μL of each concentration added to each well of a 96-well round bottom microtiter plate. Later, 97.5 μL of bacterial suspension was added to each well containing the test compound along with appropriate controls. The plates were incubated at 37 °C for 18-24 h following which the growth was enumerated and MIC was identified. The MIC is defined as the lowest compound concentration where there is no visible growth. For each compound, MIC determinations were carried independently three times using duplicate samples.

Bacterial time-kill kinetics

The presence or absence of bactericidal activity was assessed by the time-kill method.[S10,S11] Briefly, *S. aureus* ATCC 29213 bacteria were diluted ~10^6 CFU/mL in MHB and treated with

1X and 10X of MIC of complex **1** and vancomycin and incubated at 37 °C with shaking for 24 h. 100 μL samples were collected at the time intervals of 0, 1, 6 and 24 h, serially diluted in PBS and plated on MHA followed by incubation at 37 °C for 18-20 h. The time-kill curves were constructed by counting the colonies from plates and plotting the CFU/mL of surviving bacteria at each time point in the presence and absence of compound. Each experiment was repeated three times in duplicate and the mean data is plotted.

Drug interaction with FDA approved drugs

Interaction of **1** with FDA approved drugs namely ceftazidime, daptomycin, gentamycin, linezolid, levofloxacin, meropenem, minocycline, rifampicin, and vancomycin was tested by the checkerboard method. Serial two-fold dilutions of each drug were freshly prepared prior to testing. The complex **1** was two-fold diluted along the abscissa while the antibiotics were serially diluted along the ordinate in 96 well microtiter plate. 95 μL of ~10^6 CFU/mL was added to each well and plates were incubated at 37 °C for 24 h. After the incubation, the ΣFICs (fractional inhibitory concentrations) were calculated as follows: ΣFIC = FIC A + FIC B, where FIC A is the MIC of drug A in the combination/MIC of drug A alone and FIC B is the MIC of drug B in the combination/MIC of drug B alone. The combination is considered synergistic when the ∑FIC is ≤0.5, indifferent when the ∑FIC is >0.5 to 4, and antagonistic when the ∑FIC is >4.[S12]

Determination of activity against *S. aureus* biofilm

The determination of anti-biofilm activity of the tested compound was performed as described in literature.[S13] Briefly, *S. aureus* ATCC 29213 were grown overnight in 1% TSB with shaking (180 RPM) at 37 °C. The overnight culture was diluted in fresh TSB broth (1:100) and 0.2 mL of freshly diluted culture was transferred into 96 well polystyrene flat bottom plate, covered with adhesive foil lid for maintaining low oxygen and incubated in static condition for 48 h at 37 °C. After incubation, media was decanted and the plate was rinsed gently three times with the 1X PBS (pH 7.4) to remove the planktonic bacteria. Plates were refilled with TSB with different drug concentration and incubated for 24 h at 37 °C. After drug treatment, the media was decanted, washed three times with 1X PBS (pH 7.4) and biofilm was fixed by incubating the plate at 60 °C for 1 h. After fixing, the biofilm is stained by 0.06% crystal violet for 10 minutes,

rinsed with PBS and dried at room temperature. For quantification of biofilm, the bound crystal violet was eluted by 30% acetic acid (0.2 mL). Absorbance was taken on microtiter plate reader at 600 nm for biofilm quantification.

Murine neutropenic thigh infection model

For *in vivo* evaluation of antimicrobial activity of **1**, male BALB/C mice weighing ~20-24 gm were rendered neutropenic by intraperitoneally (IP) administered cyclophosphamide injections (100 mg/kg of body weight) given 24 h and 1 h before infection.[S14, S15] Following induction of neutropenia, the thigh of mice was infected with ~10^9 CFU of *S. aureus* ATCC 29213. 3 h post-infection, **1** and vancomycin, each at 25 mg/kg body weight, were injected IP into mice, twice at an interval of 3 h between injections. Control animals were administered saline in the same volume and frequency as those receiving treatment. After 24 h, the mice were sacrificed, thigh tissue was collected, weighed and homogenized in 5 mL of saline. The homogenate was serially diluted and plated on MHA plates for CFU determination. After incubation for 18–24 h at 37 °C, CFU were enumerated and the data was averaged across three experiments.

Cell cytotoxicity assay

Cell toxicity was performed against Vero cells using the MTT assay.[S16] ~10^3 cells/well were seeded in 96 well plate and incubated at 37 °C in 5% CO_2 atmosphere. After 24 h, compound was added ranging from 100-12.5 μg/mL concentration and incubated for 72 h. After the incubation was over, MTT was added in each well, incubated at 37 °C for further 4 h, residual medium was discarded, 0.1 mL of DMSO was added to solubilise the formazan crystals and OD was taken at 540 nm for the calculation of CC_{50}. CC_{50} is defined as the lowest concentration of compound which leads to a 50% reduction in cell viability. Doxorubicin was used as positive control and each experiment was repeated in triplicate.

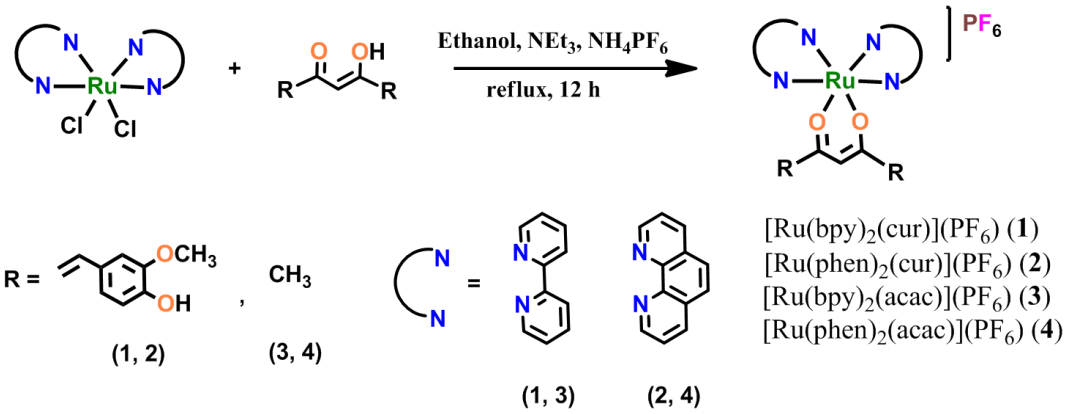

Scheme S1. General synthetic scheme for the preparation of the complexes **1**-**4**.

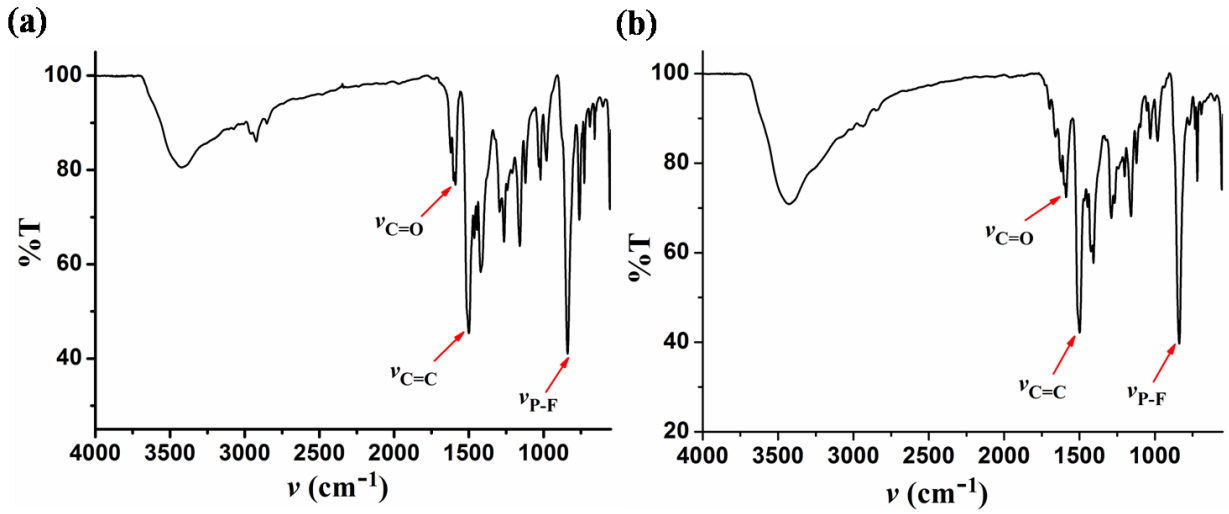

Figure S1. FTIR spectrum of [Ru(bpy)$_2$(cur)](PF$_6$) (**1**) and [Ru(phen)$_2$(cur)](PF$_6$) (**2**) in KBr phase, characteristic stretching frequencies were marked in the spectra.

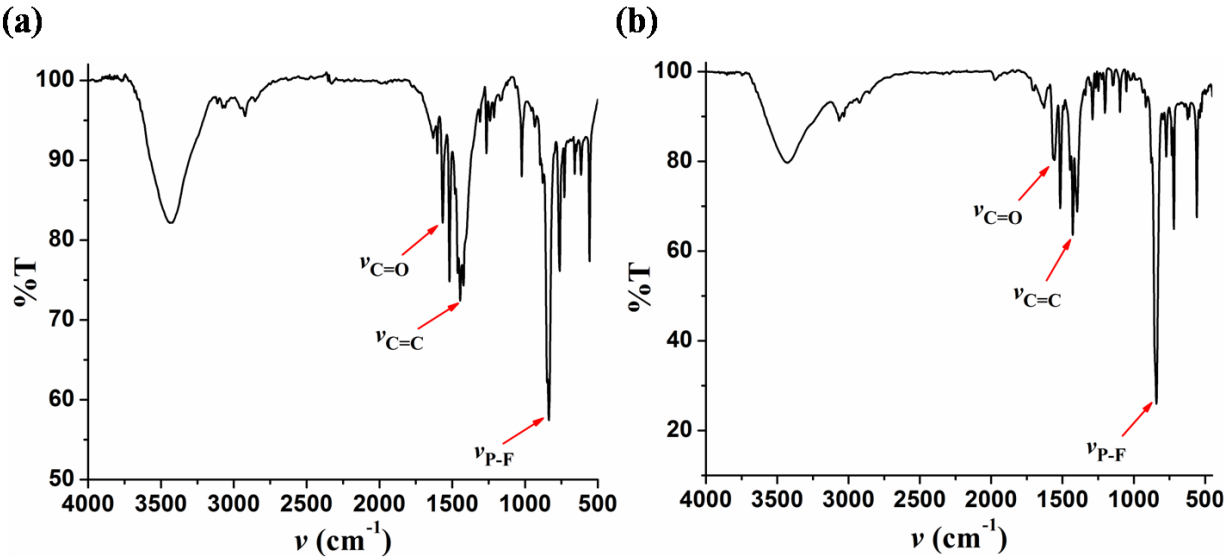

Figure S2. FT-IR spectrum of $[Ru(bpy)_2(acac)](PF_6)$ (**3**) and $[Ru(phen)_2(acac)](PF_6)$ (**4**) in KBr phase, characteristic stretching frequencies were marked in the spectra.

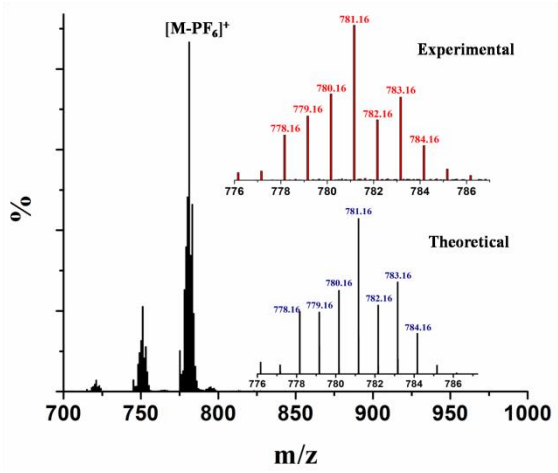

Figure S3. ESI-MS of the complex $[Ru(bpy)_2(cur)](PF_6)$ (**1**) in ethanol. Inset shows *m/z* ($[M-PF_6]^+$), calc. *m/z* for $[C_{41}H_{35}N_4O_6Ru]^+$: 781.16 (experimentally and theoretically) with matching isotopic distribution pattern.

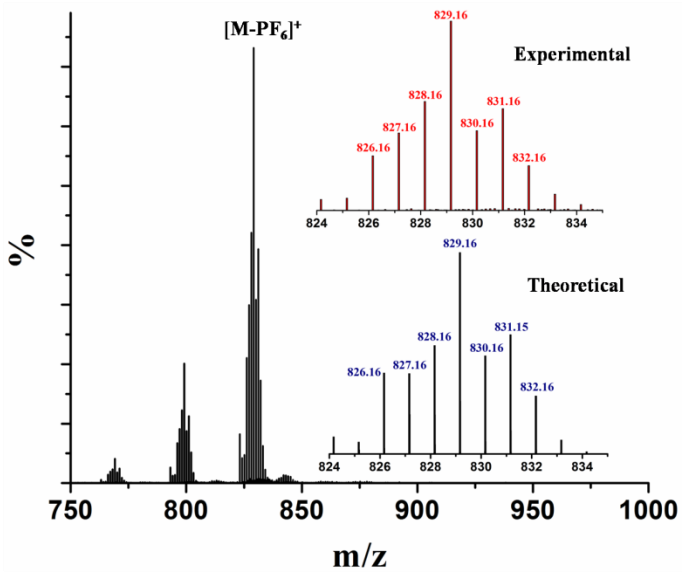

Figure S4. ESI-MS of the complex $[Ru(phen)_2(cur)](PF_6)$ (**2**) in ethanol. Inset shows *m/z* ($[M\text{-}PF_6]^+$) calc. *m/z* for $[C_{45}H_{35}N_4O_6Ru]^+$: 829.16 (experimentally and theoretically) with matching isotopic distribution pattern.

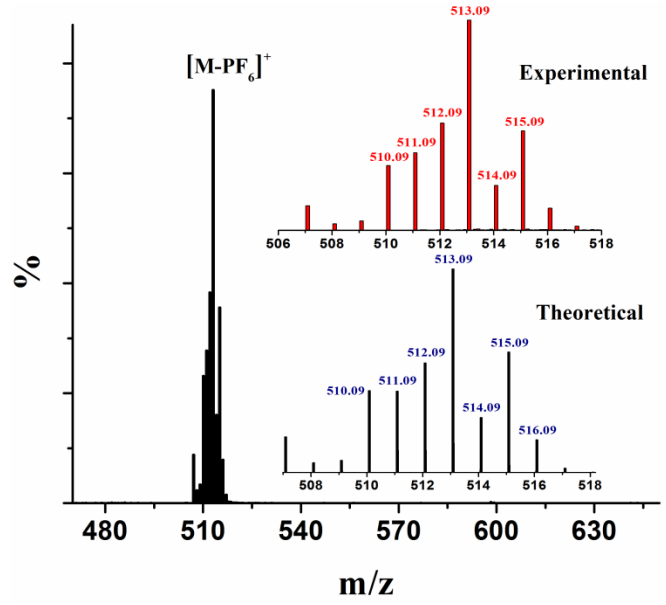

Figure S5. ESI-MS of the complex $[Ru(bpy)_2(acac)](PF_6)$ (**3**) in ethanol. Inset shows *m/z* ($[M\text{-}PF_6]^+$) calc. for $[C_{25}H_{23}N_4O_2Ru]^+$: 513.09 (experimentally and theoretically) with matching isotopic distribution pattern.

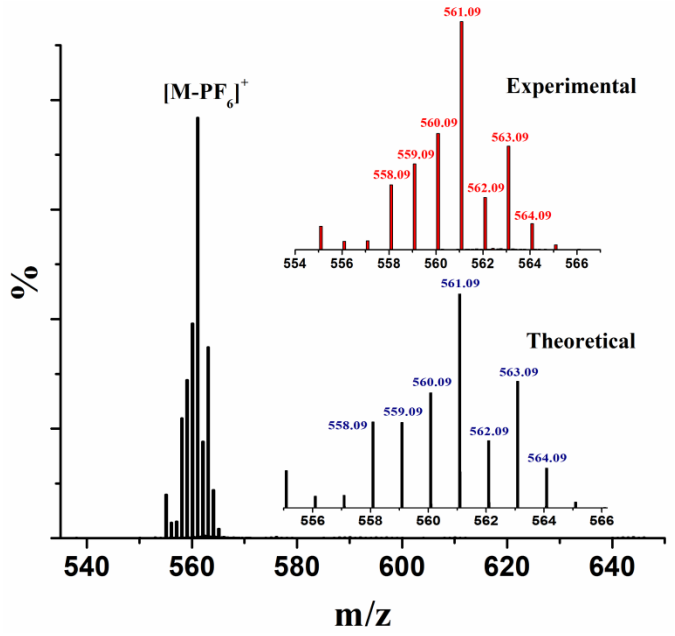

Figure S6. ESI-MS of the complex $[Ru(phen)_2(acac)](PF_6)$ (**4**) in ethanol. Inset shows *m/z* ($[M\text{-}PF_6]^+$) calc. for $[C_{29}H_{23}N_4O_2Ru]^+$: 561.09 (experimentally and theoretically) with matching isotopic distribution pattern.

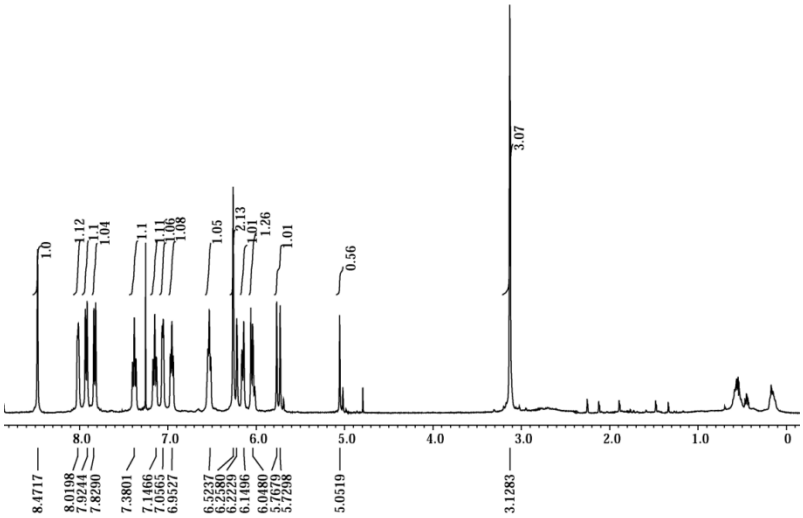

Figure S7.^{1}H NMR spectrum of complex $[Ru(bpy)_2(cur)](PF_6)$ (**1**) in $CDCl_3$ at 298 K (400 MHz) using TMS as reference.

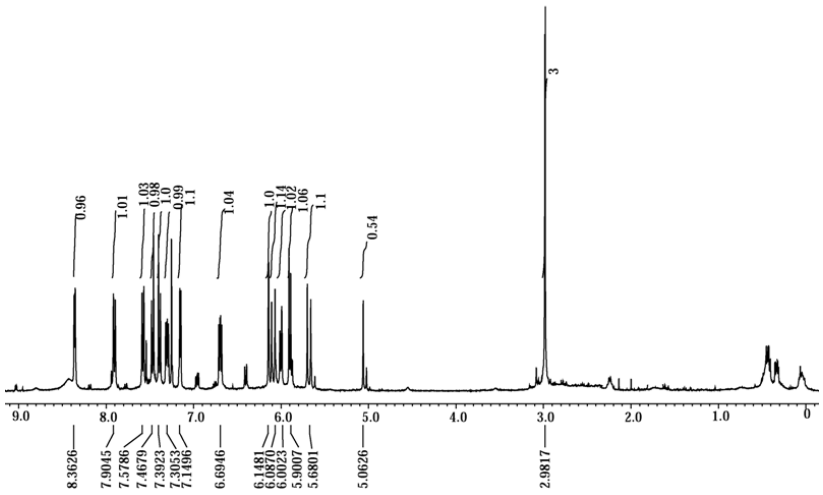

Figure S8.[1]H NMR spectrum of complex [Ru(phen)$_2$(cur)](PF$_6$) (**2**) in CDCl$_3$ at 298 K (400 MHz) using TMS as reference.

.

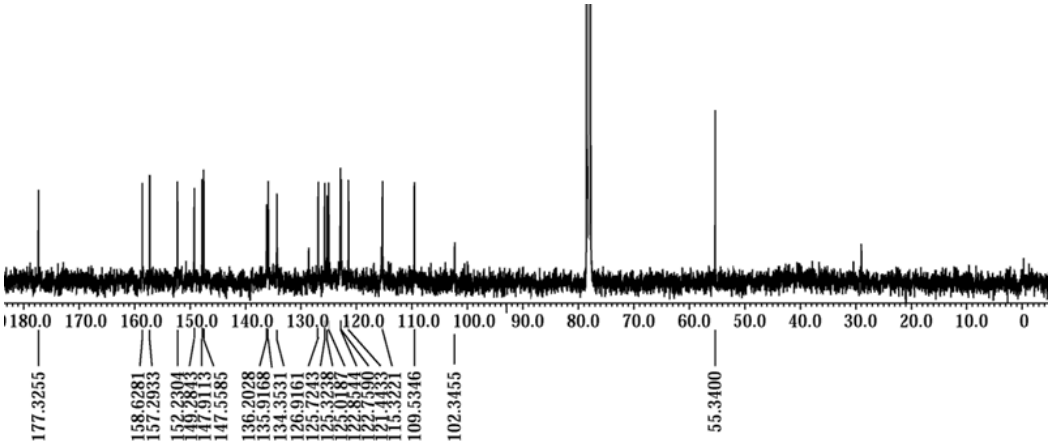

Figure S9. [13]C NMR spectrum of complex [Ru(bpy)$_2$(cur)](PF$_6$) (**1**) in CDCl$_3$ at 298 K (400 MHz) using TMS as reference.

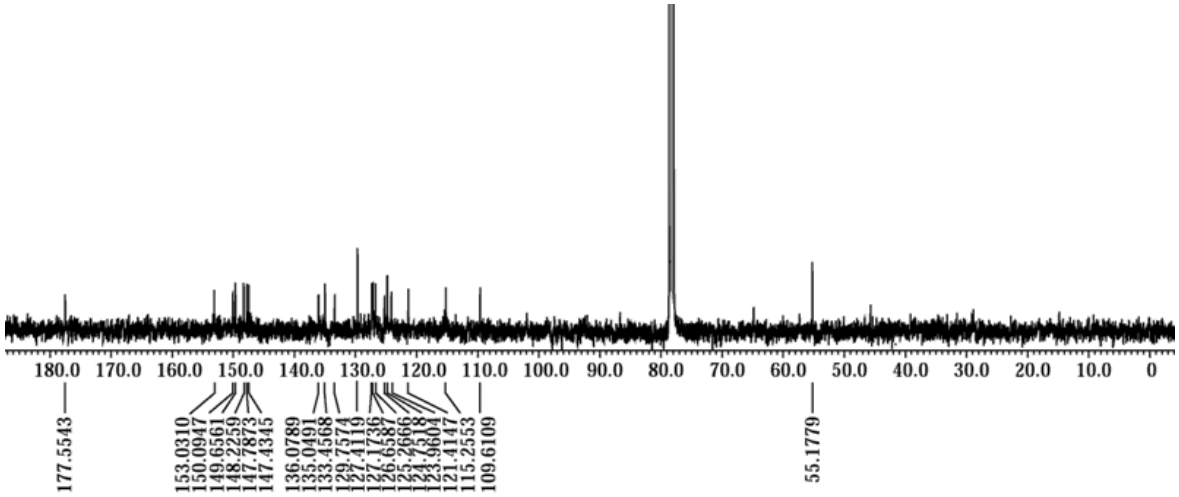

Figure S10. ^{13}C NMR spectrum of complex $[Ru(phen)_2(cur)](PF_6)$ (**2**) in $CDCl_3$ at 298 K (400 MHz) using TMS as reference.

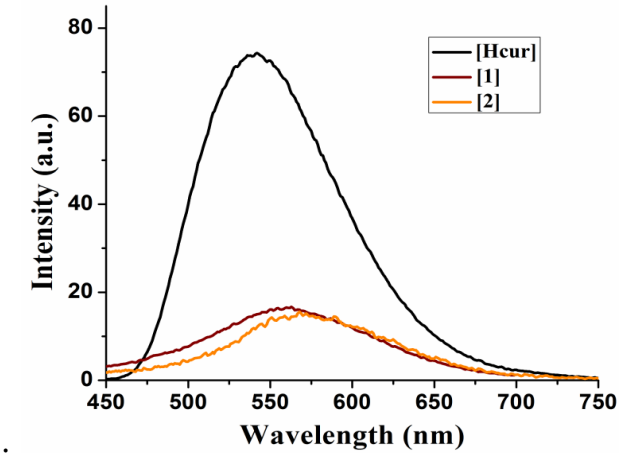

Figure S11. Emission spectra (λ_{ex}= 417 nm) of the complexes **1**, **2** and Hcur (16 μM) in ethanol at 298 K.

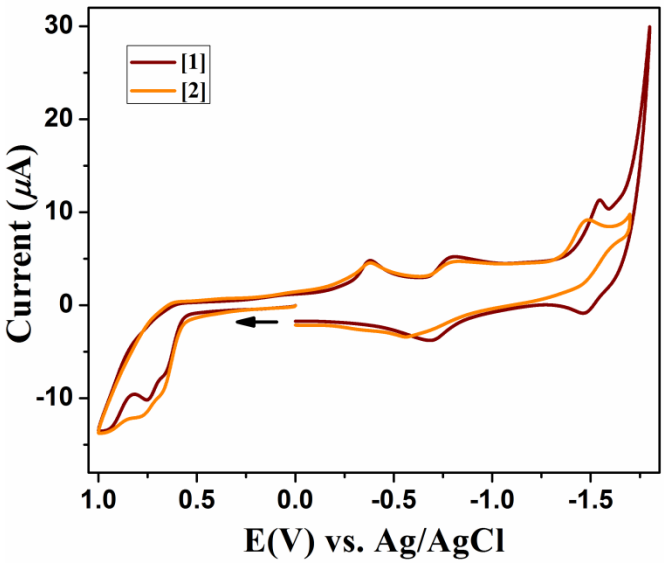

Figure S12: Cyclic voltammograms of the complexes $[Ru(bpy)_2(cur)](PF_6)$ (**1**) and $[Ru(phen)_2(cur)](PF_6)$ (**2**) in DMF and 0.1 M tertabutylammoniumhexafluorophosphate ($TBAPF_6$) as supporting electrolyte at a scan speed of 100 mV s^{-1} at 25 °C.

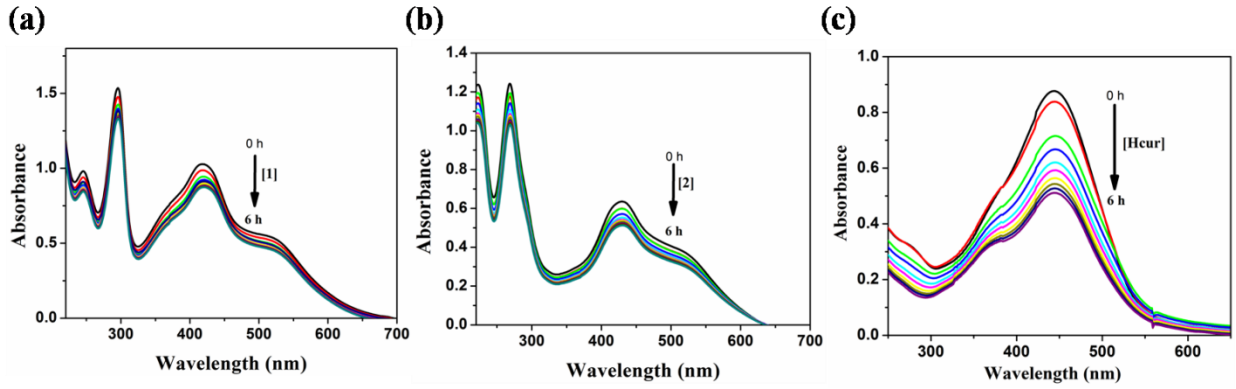

Figure S13. Time-dependent absorption spectral traces of complex **1**, **2** and Hcur monitored for 6 h in Tris buffer (pH 7.2) at 298 K.

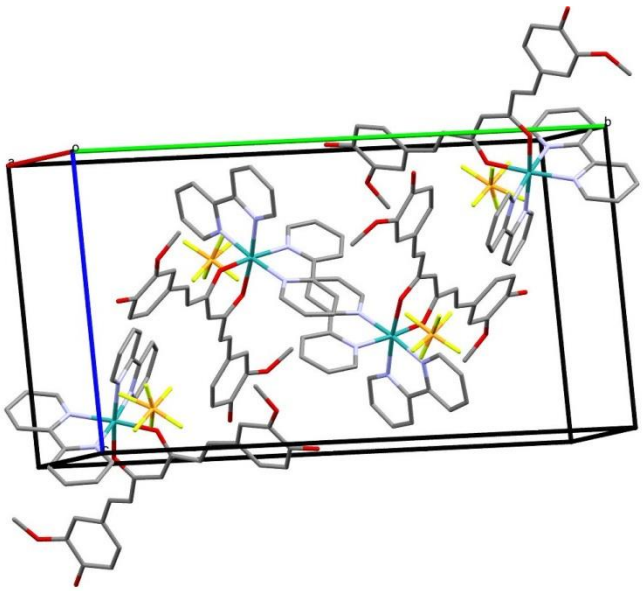

Figure S14. Unit cell packing diagram of complex $[Ru(bpy)_2(cur)](PF_6)$ (**1**).

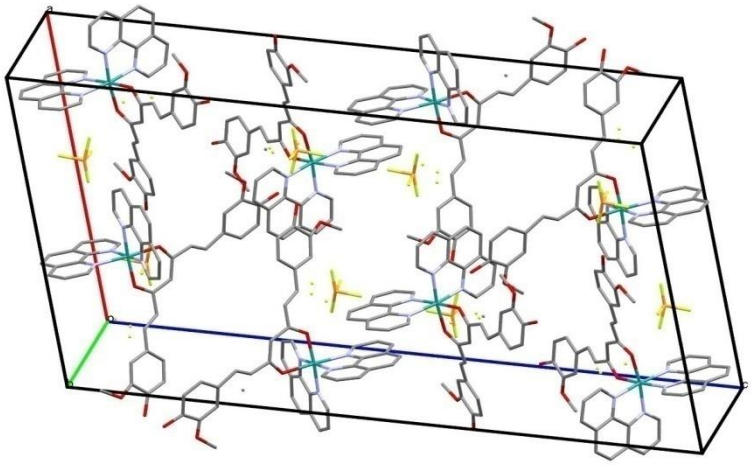

Figure S15. Unit cell packing diagram of complex $[Ru(phen)_2(cur)](PF_6)$ (**2**).

Table S1. Selected crystallographic data for complex $[Ru(bpy)_2(cur)](PF_6)$ (**1**) and $[Ru(phen)_2(cur)](PF_6)$ (**2**)

Parameters	**1**	**2**
Empirical formula	$C_{41}H_{35}F_6N_4O_6PRu$	$C_{45}H_{33}F_6N_4O_6PRu$
Formula weight	925.77	971.79
Temperature/*K*	273.15	273.15
Crystal system	monoclinic	monoclinic
Space group	$P2_1/n$	$I2/a$
a/Å	12.9304(11)	21.829(6)
b/Å	24.117(2)	11.353(3)
c/Å	13.6863(12)	37.793(10)
α/°	90.0	90.0
β/°	101.299(2)	101.698(15)
γ/°	90.0	90.0
Volume/Å^3	4185.3(6)	9172(4)
Z	4	8
ρ_{calc} g/cm^3	1.469	1.408
μ/mm^{-1}	0.490	0.451
F(000)	1880.0	3936.0
Crystal size/mm^3	0.28 × 0.24 × 0.19	0.27 × 0.23 × 0.18
2θ range for data collection/°	4.308 to 50	4.402 to 49.998
Index ranges	$-15 \le h \le 15$, $-28 \le k \le 28$, $-16 \le l \le 16$	$-25 \le h \le 25$, $-13 \le k \le 13$, $-44 \le l \le 44$
Reflections collected	44712	45704
Independent reflections	7363 [R_{int} = 0.0589, R_{sigma} = 0.0486]	8066 [R_{int} = 0.1467, R_{sigma} = 0.1024]
Data/restraints/parameters	7363/175/500	8066/211/549
Goodness-of-fit on F^2	1.748	1.036
R_1[a] and wR_2[b] [[I>=2σ (I)]	0.1476, 0.4305	0.1248, 0.3225
R_1 and wR_2 [all data]	0.1971, 0.4740	0.1750, 0.3656
Largest diff. peak/hole /e Å^{-3}	2.29/-1.85	1.70/-1.60
CCDC No.	1873397	1873398

[a] $R1=\Sigma||F0|-|FC||/\Sigma|F0|$; [b] $wR^2=\{\Sigma[w(F0^2-FC^2)]/\Sigma[w(F0^2)^2]\}^{1/2}$

Table S2. Selected bond lengths (Å) and angles (°) of $[Ru(bpy)_2(cur)](PF_6)$ (**1**) and $[Ru(phen)_2(cur)](PF_6)$ (**2**) with e.s.d.s. in parentheses.

Bond distance (1)		**Bond distance (2)**	
Ru(1)-O(4)	2.049(9)	Ru(1)-O(3)	2.067(8)
Ru(1)-O(3)	2.032(7)	Ru(1)-N(1)	2.063(9)
Ru(1)-N(3)	2.048(9)	Ru(1)-N(2)	2.063(9)
Ru(1)-N(4)	2.029(9)	Ru(1)-N(4)	2.059(10)
Ru(1)-N(1)	2.066(10)	Ru(1)-N(3)	2.059(9)
Ru(1)-N(2)	2.028(11)	Ru(1)-O(4)	2.078(8)
Bond angles (1)		**Bond angles (2)**	
O(4)-Ru(1)-N(1)	174.0(5)	O(3)-Ru(1)-O(4)	91.5(3)
O(3)-Ru(1)-O(4)	91.7(3)	N(1)-Ru(1)-O(3)	92.8(3)
O(3)-Ru(1)-N(3)	171.5(5)	N(1)-Ru(1)-O(4)	92.8(3)
O(3)-Ru(1)-N(1)	85.2(3)	N(2)-Ru(1)-O(3)	89.7(3)
N(3)-Ru(1)-O(4)	90.4(4)	N(2)-Ru(1)-N(1)	80.2(4)
N(3)-Ru(1)-N(1)	93.3(4)	N(2)-Ru(1)-O(4)	172.9(3)
N(4)-Ru(1)-O(4)	90.9(3)	N(4)-Ru(1)-O(3)	171.9(3)
N(4)-Ru(1)-O(3)	91.9(3)	N(4)-Ru(1)-N(1)	95.3(3)
N(4)-Ru(1)-N(3)	79.9(5)	N(4)-Ru(1)-N(2)	92.2(3)
N(4)-Ru(1)-N(1)	94.3(6)	N(4)-Ru(1)-O(4)	87.6(4)
N(2)-Ru(1)-O(4)	94.2(5)	N(3)-Ru(1)-O(3)	91.4(3)
N(2)-Ru(1)O(3)	90.0(4)	N(3)-Ru(1)-N(1)	174.2(4)
N(2)-Ru(1)-N(3)	98.0(5)	N(3)-Ru(1)-N(2)	95.8(4)
N(2)-Ru(1)-N(4)	174.5(5)	N(3)-Ru(1)-N(4)	80.5(4)
N(2)-Ru(1)-N(1)	80.7(6)	N(3)-Ru(1)-O(4)	91.1(4)

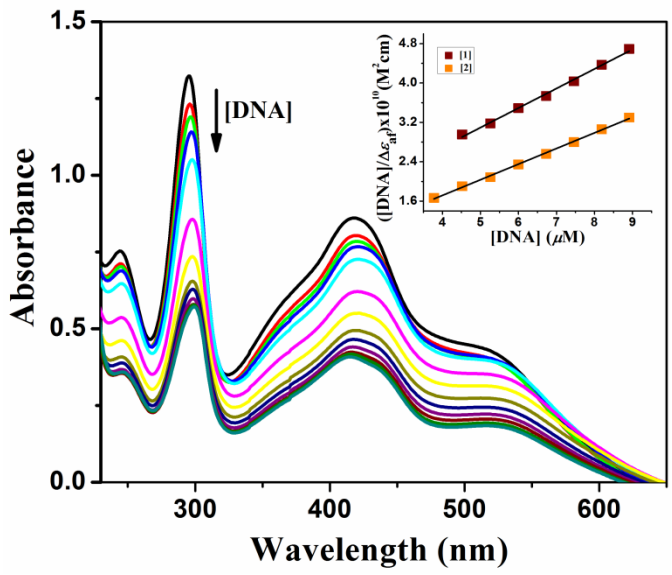

Figure S16. Absorption spectral trace of complex **1** (28 μM) in 5 mM Tris-HCl/NaCl buffer (pH 7.2) on increasing the quantity of CT-DNA at 298 K. Inset: [DNA] versus {[DNA]/($\Delta\varepsilon_{af}$)}.

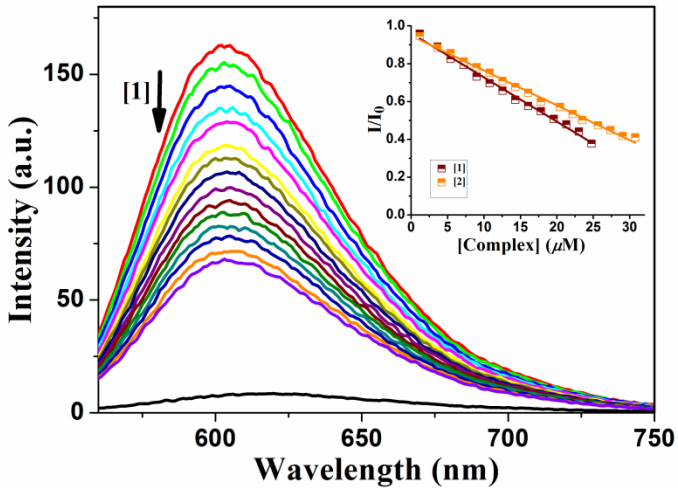

Figure S17. Emission spectra of EB in presence of complex **1** in 5 mM Tris-HCl/NaCl (pH 7.2) buffer bound to DNA, [DNA] = 25 μM, [EB] = 12 μM, λ_{ex} = 546 nm. Inset: I/I_0 vs. [Complex]

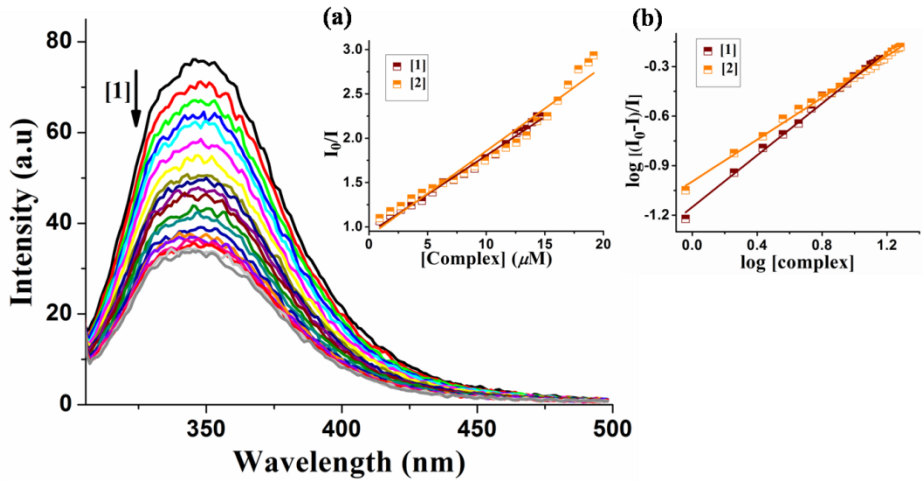

Figure S18. Emission spectral traces of human serum albumin (HSA) protein (4 μM) in the presence of complex **1**. The inset shows the (a) plot of (I_0/I) vs. [complex] (μM) and (b) Scatchard plot for log ([I_0- I]/I) vs. log[complex] for complex **1** and **2**.

Table S3. HSA binding parameters for interaction of complexes 1 and 2

Complex	K_{SV}[a]/M^{-1}	k_q[b]/M^{-1} s^{-1}	K[c] /M^{-1}	n[d]
1	0.94 x 10^5	0.94 x 10^{13}	1.15 x 10^6	0.78
2	1.07 x 10^5	1.07 x 10^{13}	0.99 x 10^6	0.63

[a]K_{SV}, Stern-Volmer quenching constant. [b]k_q, quenching rate constant. [c]K, binding constant. [d]n, number of binding sites.

Table S4. Minimum Inhibitory Concentrations (μg mL^{-1}) of 1, 2 and control antibiotics against clinical MRSA and VRSA strains

	MSSA	VRSA			MRSA								
Compounds	***S.aureus*** **ATCC 29213**	***S.aureus*** **VRS 1**	***S.aureus*** **VRS 4**	***S.aureus*** **VRS 12**	***S.aureus*** **NRS 100**	***S.aureus*** **NRS 119**	***S.aureus*** **NRS 129**	***S.aureus*** **NRS 186**	***S.aureus*** **NRS 191**	***S.aureus*** **NRS 192**	***S.aureus*** **NRS 193**	***S.aureus*** **NRS 194**	***S.aureus*** **NRS 198**
1	1	1	1	2	1	1	1	1	1	1	2	1	1
2	1	1	1	1	1	1	1	1	1	1	2	1	1
Levofloxacin	0.25	64	>64	64	0.25	16	0.25	8	32	8	32	0.25	32
Meropenem	0.5	>64	>64	32	>64	>64	32	32	>64	64	>64	8	>64
Methicillin	2	>64	>64	64	>64	>64	64	64	>64	>64	>64	16	>64
Vancomycin	1	>64	>64	>64	2	2	1	2	2	1	2	1	2

Table S5. Fractional inhibitory concentrations (FIC) indexes of synergy of 1 with approved antibiotics utilized for the treatment of *S. aureus* infections

Compounds	MIC (μgmL^{-1})	MIC of 1 in the presence of drug (μgmL^{-1})	MIC of drug in the presence of 1 (μgmL^{-1})	FIC A	FIC B	∑FIC (FIC A +FIC B)	Inference
1	2						
Ceftazidime	16	1	8	0.5	0.5	1	No interaction
Daptomycin	0.5	1	0.25	0.5	0.5	1	No interaction
Gentamycin	0.25	1	0.125	0.5	0.5	1	No interaction
Linezolid	2	1	1	0.5	0.5	1	No interaction
Levofloxacin	0.25	1	0.125	0.5	0.5	1	No interaction
Meropenem	0.5	1	0.0018	0.5	0.0036	0.5	Synergistic
Minocycline	0.125	1	0.0018	0.5	0.0144	0.5	Synergistic
Rifampicin	0.00037	1	0.00003	0.5	0.081081	0.5	Synergistic
Vancomycin	1	1	0.0039	0.5	0.0039	0.5	Synergistic

References

1 A. M. El-Hendawy, A. H. Al-Kubaisi, H. A. Al Madfa, *Polyhedron*, 1997, **16**, 3039-3045.

2 APEX2 v2012.4, Bruker AXS, Madison, WI, 1999.

3 G. M. Sheldrick, SHELX-97, Program for Refinement of Crystal Structures, University of Göttingen, Göttingen, Germany, 1997.

4 G. M. Sheldrick, SHELXTL 6.14, Bruker, AXS Inc., Madison, WI, 2000.

5 A. Wolfe, G. H. Shimer, T. Meehan, *Biochemistry*, 1987, **26**, 6392-6396.

6 M. Lee, A. L. Rhodes, M. D. Wyatt, S. Forrow, J. Hartley, *Biochemistry*, 1993, **32**, 4237-4245.

7 J. R. Lakowicz, *Principles of Fluorescence Spectroscopy*, third ed., Springer, New York, 2006.

8 G. Scatchard, *Ann. N. Y. Acad. Sci*., 1949, **51**, 660-672.

9 P. A. Wayne, *Clinical and Laboratory Standards Institute*, **2012**, 8thed.

10 K. V. Sashidhara, K. B. Rao, P. Kushwaha, R. K. Modukuri, P. Singh, I. Soni, P. K. Shukla, S. Chopra, M. Pasupuleti, *ACS Med. Chem. Lett.*, 2015, **6**, 809-813.

11 P. A. Wayne, NCCLS document M26-A. *National Committee for Clinical Laboratory Standards* 1999, **19**.

12 F. C. Odds, *J. Antimicrob. Chemother*., 2003, **52**, 1.

13 S. M. Kwasny, T. J. Opperman, *Curr. Protoc. Pharmacol*., 2010, 1-27.

14 J. Wang J, Q. Shan, H. Ding, C. Liang, Z. Zeng, *Antimicrob. Agents Chemother.*, 2014, **58**, 3008-3012.

15 W. A. Craig, J. Redington, S. C. Ebert, *J. Antimicrob. Chemother*., 1991, **27**, 29–40.

16 P. R. Twentyman, M. A. Luscombe, *Br. J Cancer*, 1987, **56**, 279-285.